Growth Behavior of Crystal Faces Containing Symmetry-Related Connected Nets: A Case Study of Naphthalene and Anthracene

R. F. P. Grimbergen, M. F. Reedijk, H. Meekes,* and P. Bennema

RIM Laboratory of Solid State Chemistry, Faculty of Science, University of Nijmegen, Toernooiveld 1, 6525 ED Nijmegen, The Netherlands

Received: October 31, 1997; In Final Form: February 3, 1998

The morphology of naphthalene and anthracene crystals has been studied both theoretically and experimentally. A connected net analysis shows that the faces {011} and $\{2\bar{1}\bar{1}\}$ contain a pair of symmetry-related connected nets giving rise to a new phenomenon called symmetry roughening. Experimentally the {011} and $\{2\bar{1}\bar{1}\}$ faces have only been observed on naphthalene crystals grown from the vapor at very low driving forces. Upon increasing the driving force, the {011} faces grow out very rapidly as flat faces at very low supersaturation. For anthracene these faces have never been observed. In this paper the relation between the connected net structure of crystal faces and the experimentally observed growth behavior is discussed.

1. Introduction

It is a well-known fact that the morphology of crystals depends on growth conditions such as temperature, driving force, and mother phase. All these parameters influence the morphology and growth behavior of crystal faces (*hkl*).

In this paper the morphology of crystals will be studied for crystals grown from the vapor and from solution as a function of driving force in order to determine both the influence of a mother phase and the driving force. The observed crystal habits will be compared with theoretically calculated morphologies. In this way the predictive value of the recently developed extension of the Hartman−Perdok theory, which takes the effect of multiple connected nets for a crystal face (*hkl*) on the crystal morphology into account, is tested.[1−3]

Naphthalene and anthracene have been chosen as model compounds because they have been studied extensively in the past[4−7] and crystals can be grown easily both from the vapor and solution. The reason to choose both naphthalene and anthracene is that these compounds have a similar crystal structure. The only difference is that the interactions (or bond energies) in the lattice are slightly different. Therefore, the relation between the interactions in the lattice and the macroscopic morphology can be studied directly.

The Hartman−Perdok theory[8−11] combined with the theory of roughening transitions in relation to connected nets[1,12−14] has been used to predict the crystal morphology. To derive a crystal habit from a crystal structure, first the most important bonds or interactions between growth units in the lattice have to be determined. The interactions between the growth units are calculated using an empirical force field. Bonds having a bond energy larger than the thermal energy kT (T is the actual growth temperature) are used in the analysis. The growth units are subsequently reduced to their corresponding centers of geometry. The centers of geometry connected by the bonds define a so-called crystal graph. From the crystal graph first all direct chains (DCs) are derived. A DC is defined as a sequence of strongly bonded growth units of which only the end points are identical (i.e., related by a lattice translation $[uvw]$ with $u, v, w \in Z$). A connected net (*hkl*) perpendicular to $\boldsymbol{k}_{hkl} = h\boldsymbol{a}^* + k\boldsymbol{b}^* + l\boldsymbol{c}^*$ is a combination of at least two nonparallel intersecting DCs $[uvw]_1$ and $[uvw]_2$ perpendicular to $\boldsymbol{k}_{hkl}$. Moreover, all equivalent growth units of a connected net differ by a translation $[uvw]$ perpendicular to $\boldsymbol{k}_{hkl}$. Given the space group, symmetry equivalent connected nets are separated by the interplanar distance d_{hkl} according to the selection rules of Bravais, Friedel, Donnay, and Harker (BFDH).[1,15,16] Note that a connected net need not be stoichiometric with regard to the chemical composition of the unit cell. Therefore, only stoichiometric connected nets can be considered as the actual growth layers with which a crystal will grow.

In equilibrium a flat face or F-face (i.e., a crystal face below the roughening temperature) with normal $\boldsymbol{k}$ has the property that for all crystallographic directions $\boldsymbol{u} = u\boldsymbol{a} + v\boldsymbol{b} + w\boldsymbol{c}$ labeled by $[uvw]$ ($u, v, w \in$ Z) coplanar with the face (i.e., $\boldsymbol{u}\cdot\boldsymbol{k} = 0$) the sum of the edge free energies of a step in the $\boldsymbol{u}$ and $-\boldsymbol{u}$ direction is larger than zero,[17] or

$$\gamma(\boldsymbol{u}) + \gamma(-\boldsymbol{u}) > 0 \qquad \forall \boldsymbol{u}, \boldsymbol{u}\cdot\boldsymbol{k} = 0 \tag{1}$$

In the case where eq 1 also holds for a single connected net of a face, it can be seen that for that net the step free energy will be larger than zero for all directions $\boldsymbol{u}$ and $-\boldsymbol{u}$. It has been shown that a connected net has a 2-D Ising transition temperature T^{C}_{hkl}, and this temperature has been used as a rough estimate for the roughening temperature T^{R}_{hkl} of the crystal face (*hkl*).[12] More specifically it has been assumed that the 2-D Ising transition temperature of the strongest connected net for a crystal face (*hkl*) is an (usually lower bound) estimate of the roughening temperature. Recently, it has been demonstrated that this assumption is not valid in general. Combinations of connected nets may result in a very low or even zero step energy for a face (*hkl*).[1]

To determine the growth morphology based on F-faces, Hartman and Bennema introduced the attachment energy as a habit-controlling factor.[18] The attachment energy is defined as the energy released per growth unit when a complete growth layer (i.e., stoichiometric connected net) is attached to the surface (*hkl*) of a crystal. The attachment energy is related to the crystallization energy by

S1089-5647(98)00040-6 CCC: $15.00
Published on Web 03/24/1998

$$E^{cr} = E^{att}_{hkl} + E^{slice}_{hkl} \quad (2)$$

where E^{slice}_{hkl} is the interaction energy of all growth units within the stoichiometric connected net or growth layer. It was argued that it may be justified that the relative growth rates of crystal faces are proportional to the attachment energy or

$$R_{hkl} \propto E^{att}_{hkl} \quad (3)$$

Subsequently, a Wulff plot can be used to construct the growth morphology.[19]

In this paper we will demonstrate that the combination of (symmetry-related) connected nets, each having a very high Ising transition temperature, may result in an overall zero step energy for the crystal face (*hkl*) and thus a roughening temperature of 0 K. Such a situation is known as symmetry roughening.[1,2] For such faces the attachment energy is not a good parameter to determine the growth rate of the face and relation 3 does not hold. Moreover, even for faces that contain no symmetry-related connected nets, but a pair of connected nets causing a very low step energy, the attachment energy is not a reliable measure for the growth rate.[1,3] Obviously, this has major implications for the equilibrium and growth behavior of these specific faces. The {011} and $\{2\bar{1}\bar{1}\}$ faces of naphthalene and anthracene are examples of such faces. Experimental observations support the theoretical results.

2. Theoretical Morphology

The connected nets have been derived from the crystal graph using the program FACELIFT[20] based on the graph-theoretical method described by Strom.[21−23] Point charges for the atoms of both naphthalene and anthracene have been calculated from the electron densities determined with GAMESS[24] using the 6-31G** basis and D_{2h} molecular symmetry. The electrostatic potential derived (ESPD) point charges were subsequently calculated from the electron densities using the program MOLDEN.[25,26] Bond energies needed for calculation of the 2-D Ising transition temperatures and attachment energies have been calculated using the Cerius[2] software.[27] The 2-D Ising transition temperatures of connected nets have been calculated using the program TCRITIC.[12,28] Note that we use the term bond energy for the energy of the intermolecular interactions between the growth units.

2.1. Crystal Graph. Naphthalene and anthracene crystallize in space group $P2_1/a$ with two molecules in the unit cell with geometrical centers M_1 at (0, 0, 0) and M_2 at ($^1/_2$,$^1/_2$, 0).[29,30] The cell parameters are given in Table 1. To determine the interplanar distance d_{hkl} separating physically equivalent surface structures, the selection rules for (*h*0*l*) $h = 2n$ and for (0*k*0) $k = 2n$ for spacegroup $P2_1/a$ have been applied.[31]

Because the crystal structures of naphthalene and anthracene are very similar, a generalized crystal graph can be used to determine all connected nets for both crystals. The crystal graph used in this study was based on the work of Hartman, who derived a general crystal graph for organic compounds having two centrosymmetric molecules in the unit cell,[32] and on the work of Bennema on naphthalene (see review paper ref 14). In the present study the *p*, *q*, *r*, and *s* bond types used by Hartman (*a*, *d*, *f*, and *g* bond types of Bennema) and an additional bond *v* have been used. The broken bond energies of these bonds are larger than *kT*. The *t* bond used by Hartman appeared to be very weak (≈0.3 *kT*) and was omitted in this work. In the following the broken bond energies of these bonds will be indicated with Φ_p, Φ_q, Φ_r, Φ_s, and Φ_v. Hartman applied an extra selection rule for (*hkl*), $h + k = 2n$, to determine the F-faces which has not been used in this work. An explanation for this choice will be given further on.

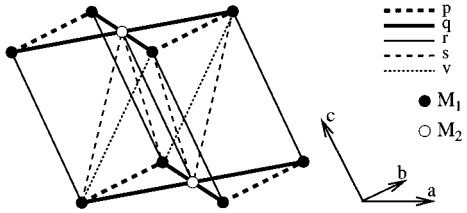

Figure 1. Crystal graph with the bonds defined in Table 2.

TABLE 1: Cell Parameters and Lattice Energies of Naphthalene and Anthracene before and after Minimization. CSD Indicates the Cell Parameters Obtained from the Cambridge Structural Database

	naphthalene		anthracene	
	CSD	minimized	CSD	minimized
a (Å)	8.213	8.138	8.553	8.483
b (Å)	5.973	6.043	6.016	6.045
c (Å)	8.674	8.748	11.172	11.141
β	123.39	123.71	124.60	124.40
E_{latt} (kcal/mol)	−18.36	−18.68	−26.64	−26.55

TABLE 2: Bonds Defining the Crystal Graph for Naphthalene and Anthracene. Broken Bond Energies Calculated for Naphthalene and Anthracene Are Given

	bond	naphthalene E^{bb} (kcal/mol)	anthracene E^{bb} (kcal/mol)
q	M_1-M_2[000]	4.591	7.008
p	M_1-M_1[010]	2.972	4.936
s	M_1-M_2[001]	1.392	1.626
r	M_1-M_1[001]	0.895	0.765
v	M_1-M_1[101]	0.580	0.661

Before interactions between the growth units were calculated, the crystal structure was minimized to remove bad contacts. This is a generally used method to reduce errors introduced by shortcomings in the force field parameters. During the minimization, the space group symmetry was imposed and the atomic positions as well as the cell parameters *a*, *b*, *c*, and β were optimized. The Ewald summation technique has been used to calculate nonbonded interactions in the lattice. The cell parameters of naphthalene and anthracene before and after minimization are given in Table 1. Lattice energies have been calculated by summation of all atom−atom pair interactions between growth units of which the geometrical center is within a cutoff radius of 30 Å; (Table 1). This method has been used by Docherty et al.[33] It can be seen that the differences between the cell parameters before and after minimization are very small. The calculated lattice energy was −18.7 kcal/mol for naphthalene and −26.6 kcal/mol for anthracene, which is in excellent agreement with the experimental values of −18.6 and −26.2 kcal/mol, respectively.[33] The small deviation of the cell parameters from the experimental values and the calculated lattice energies indicate that the force field used describes the crystal structures correctly. Therefore the minimized crystal structure was used to calculate all interactions between the growth units in the crystal lattices.

The calculated broken bond energies of the bonds between the growth units defining the crystal graph are listed in Table 2. A graphical representation of the bonds in the unit cell is drawn in Figure 1.

2.2. Connected Nets of Naphthalene and Anthracene. The results of the connected net analysis of naphthalene are presented in Table 3 and of anthracene in Table 4. The

TABLE 3: Results of the Connected Net Analysis for Naphthalene. The Form {*hkl*}, Interplanar Distance d_{hkl}, Calculated Attachment Energy (E^{att}_{hkl}), Calculated Ising Temperature (T^C), Number of Connected Nets Found, and Indication Whether the Face Is Present in the Wulff Plot (+ present; − absent) Are Given

{*hkl*}	d_{hkl} (Å)	E^{att}_{hkl} (kcal/mol)	T^C (K)	no.	Wulff plot
{001}	7.268	−11.2	1847	1	+
{110}	4.533	−22.9	965	1	+
{20$\bar{1}$}	4.104	−25.5	859	1	+
{11$\bar{1}$}	4.664	−23.5	900	1	+
{011}	4.628	−25.3	590	2	+
{200}	3.456	−28.9	498	1	−
{20$\bar{2}$}	3.704	−29.6	423	1	−
{2$\bar{1}\bar{1}$}	3.388	−29.2	370	2	−
{020}	3.002	−33.7	207	1	−

TABLE 4: Results of the Connected Net Analysis for Anthracene. The Form {*hkl*}, Interplanar Distance d_{hkl}, Calculated Attachment Energy (E^{att}_{hkl}), Calculated Ising Temperature (T^C), Number of Connected Nets Found, and Indication Whether the Face Is Present in the Wulff Plot (+ present; − absent) Are Given

{*hkl*}	d_{hkl} (Å)	E^{att}_{hkl} (kcal/mol)	T^C (K)	no.	Wulff plot
{001}	9.197	−12.2	2881	1	+
{110}	4.574	−33.4	1246	1	+
{20$\bar{1}$}	4.172	−36.3	1187	1	+
{11$\bar{1}$}	4.874	−33.6	1222	1	+
{011}	5.034	−35.6	829	2	+
{200}	3.520	−40.9	648	1	−
{20$\bar{2}$}	4.158	−41.1	617	1	+
{2$\bar{1}\bar{1}$}	3.428	−41.9	450	2	−
{020}	3.008	−49.2	203	1	−

attachment energies were calculated according to the method described by Berkovitch−Yellin, which has been implemented in Cerius^2.[27,34] Note that the calculated 2-D Ising transition temperatures in Table 3 and 4 are an estimate for the roughening temperature for the crystal face (*hkl*) in equilibrium with its vapor phase. In the Discussion it will be shown that a solvent mother phase may reduce the roughening temperatures drastically.

For the {011} and {2$\bar{1}\bar{1}$} forms two connected nets were found. Because these connected nets are symmetry related, the calculated Ising transition temperature is for both connected nets the same. In the next section the physical implications of the presence of symmetry-related connected nets will be discussed.

The predicted growth morphologies of naphthalene and anthracene based on E_{att} (eq 3) of Tables 3 and 4 are presented in Figure 2. Both morphologies exhibit the {001}, {110},{20$\bar{1}$}, {11$\bar{1}$}, and {011} forms. Anthracene has additionally the {20$\bar{2}$} form, which is for naphthalene very close to the threshold value for appearance on the Wulff plot. The morphology of anthracene is somewhat more platy as compared to the naphthalene morphology. This can be explained by the *p* and *q* bonds, which are much stronger for anthracene than for naphthalene, because of the larger anisotropy of the molecules.

2.3. Multiple Connected Nets. For the crystal faces {011} and {2$\bar{1}\bar{1}$} more than one connected net is found. These can be considered as possible growth layers. The usual procedure is to determine the connected net with the highest slice energy and consequently the lowest attachment energy. This connected net is then considered to be the actual growth layer determining the growth and equilibrium behavior of the crystal face.

However, for the {011} and {2$\bar{1}\bar{1}$} faces a special situation occurs, as already mentioned by Hartman.[32] He found that for naphthalene type of crystals having two centrosymmetric molecules in the monoclinic unit cell at special positions ((0, 0, 0) and ($^1/_2$, $^1/_2$, 0)) the situation occurs that for all faces (*hkl*) with $h + k = 2n + 1$ exactly the same surface energy is found at distances $^1/_2 d_{hkl}$ instead of d_{hkl}. For this reason Hartman introduced for these types of structure the extra selection rule (*hkl*) $h + k = 2n$. In another paper Hartman demonstrates that these faces grow relatively fast because of nucleation at a partial step with height $^1/_2 d_{hkl}$.[35]

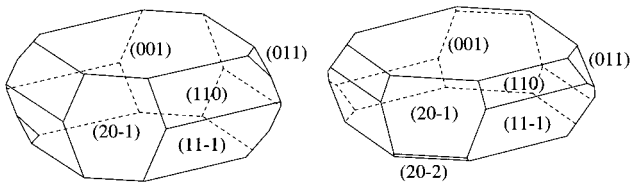

Figure 2. Calculated theoretical morphologies based on attachment energies for naphthalene (left) and anthracene (right).

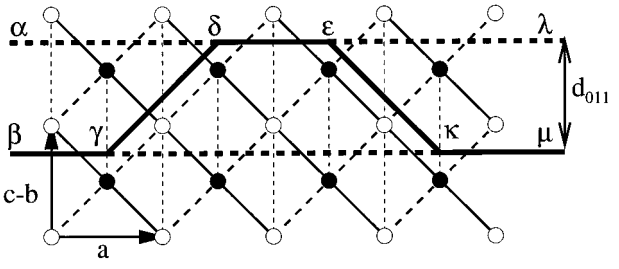

Figure 3. [0$\bar{1}$1] projection of a schematic drawing of the bonding structure for the (011) face. The open circles represent molecules 1 (M_1) and the filled circles molecules 2 (M_2). The diagonal dashed bonds represent *q* bonds, the vertical dashed bonds represent superimposed *p* and *r* bonds, and the solid bonds represent superimposed *q* and *s* bonds. The υ bonds are not drawn.

In our opinion the {011} and {2$\bar{1}\bar{1}$} faces grow very fast because of a zero step free energy in a direction [$u\upsilon w$] as a result of a pair of connected nets which are related to each other by a center of symmetry. Due to their symmetry relation the connected nets have exactly the same slice and attachment energies. This can be seen in Figure 3 for the (011) face. Note that the υ bonds are not drawn for clarity sake. These bonds do not contribute to the step energy. Looking at Figure 3, it can be seen that for the crystallographic direction $\boldsymbol{u} = [100]$ relation 1 does not hold. The broken bond step energy for [100] is equal to the difference in broken bond surface energy of the surfaces bounded by $\beta\gamma\delta\epsilon\lambda$ and $\beta\gamma\kappa\mu$. The broken bond step energy is equal to $(8\Phi_r + 8\Phi_p + 8\Phi_q + 5\Phi_s) - (8\Phi_r + 8\Phi_p + 8\Phi_q + 4\Phi_s) = \Phi_s$. For the step in the [$\bar{1}$00] direction, the corresponding surfaces are bounded by $\alpha\delta\epsilon\kappa\mu$ and $\beta\gamma\kappa\mu$. The broken bond energy for this step is $(8\Phi_r + 8\Phi_p + 8\Phi_q + 3\Phi_s) - (8\Phi_r + 8\Phi_p + 8\Phi_q + 4\Phi_s) = -\Phi_s$. Note that for the individual steps the contribution of the bonds *p*, *q*, *r*, and also υ (not drawn) to the step energy is zero. The summation of the step energies for the directions $\boldsymbol{u}$ and $-\boldsymbol{u}$ is zero. This is a special case of the condition of eq 1. Usually a face becomes rough when the step free energy becomes zero for steps in both the $\boldsymbol{u}$ and $-\boldsymbol{u}$ directions. A zero step free energy implies that there is no effective preference for a growth unit to be incorporated in a kink site or any other lattice site on the crystal surface. In this special case the step free energies of the individual step directions are nonzero but have an opposite sign. Consequently, on the basis of broken bond step energies, the roughening temperature should be 0 K (see eq 1) and the crystal face should grow in a rough mode and consequently very fast. This phenomenon was described in recent papers and called symmetry roughening.[2] For the {2$\bar{1}\bar{1}$} faces the same situation occurs.

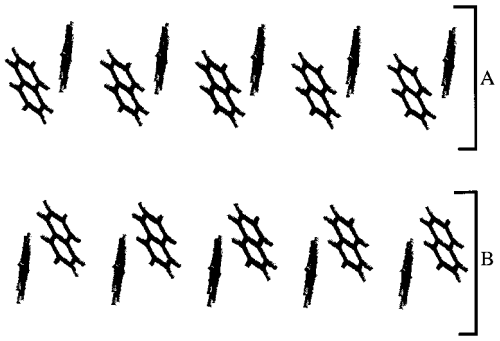

Figure 4. [$0\bar{1}1$] projection of the two surface configurations of the (011) face of naphthalene.

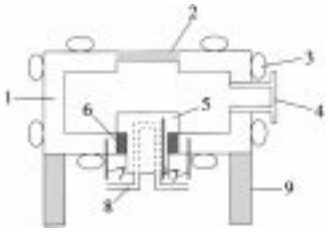

Figure 5. Schematic side view of the vapor growth cell: (1) copper cell wall, (2) glass window, (3) heating flow tubes, (4) vacuum flange, (5) cold finger, (6) thermally insulating ring, (7) thermocouple, (8) heating tubes, (9) support.

In Figure 4 it can be seen that the two connected nets represent different surface configurations. The molecules at the crystal−mother phase interface of the two surfaces indicated with A and B have different orientations with respect to the surface. For this reason the surface *free* energy of the two surface configurations will be different because of a difference in molecular entropy or due to surface relaxation. In the bonding structure of the (011) face the surface free energy and step free energy cannot be treated independently. Consequently, the step free energy will be larger than zero in the case where the entropy term for the surface free energy is taken into account and the face will have a roughening temperature larger than 0 K. For this reason it is expected that the {011} and {$2\bar{1}\bar{1}$} faces might occur on the morphology of naphthalene type of crystals at equilibium conditions. Because of the low step free energy, the faces will grow very rapidly when a driving force is applied and disappear from the morphology.[3]

Note that the 2-D Ising transition temperatures of connected nets are not a good approximation for the roughening temperature of these types of face, where a pair of connected nets causes a very low step energy.

3. Experimental Section

3.1. Vapor Growth. The crystal growth experiments were carried out in a specially designed vapor growth cell, as shown in Figure 5. The cell consists of two main parts, a cold finger and a copper wall. Crystals sublime at the cell wall, and crystals grow on the cold finger. The temperature difference between these two parts can be controlled using thermostated baths. The temperature is measured with three thermocouples (copper/constantan) of type T, one in the cold finger and two in the cell wall. The crystals can be observed in situ with a microscope via the glass window. To prevent the crystals from nucleating on the window, a screen heater has been attached to the window. The pressure in the cell can be measured by a vacuum gauge.

After evacuating the cell for one night at 70 °C to remove air and water, naphthalene or anthracene p.a. quality is put into the cell and the cell is evacuated again. The cell is connected to two separate thermostated baths to control the temperature of the cell wall and the cold finger independently. The temperature of the cold finger was kept at a constant temperature (T_0) of 283.2 K for naphthalene and 326.5 K for anthracene. The supersaturation was imposed by increasing the temperature of the copper outer wall (T) of the vapor growth cell.

TABLE 5: Results of the Vapor Growth Experiments of Naphthalene and Anthracene. + Indicates That the Face Was Always Present; +/− Indicates That the Face Has Been Found Sometimes; − Indicates That the Face Has Never Been Observed

	naphtalene			anthracene		
form	low $\Delta\mu/kT$	high $\Delta\mu/kT$	$(\Delta\mu/kT)^{cr}$ (%)	low $\Delta\mu/kT$	high $\Delta\mu/kT$	$(\Delta\mu/kT)^{cr}$ (%)
{001}	+	+	−	+	+	−
{110}	+	+	−	+	+	−
{20$\bar{1}$}	+	+	−	+	+	−
{11$\bar{1}$}	+	−	3.8	+	−	1.8
{011}	+/−	−	0.2	−	−	−
{20$\bar{2}$}	+/−	−	0.2−3.8	−	−	−
{21$\bar{1}$}	+/−	−	0.2−3.8	−	−	−
{1$\bar{1}$2}	+/−	−	0.2−3.8	−	−	−

The supersaturation in the vapor growth cell has been calculated assuming ideal gas behavior using[36]

$$\frac{\Delta\mu}{kT_0} = \ln\frac{T}{T_0} \tag{4}$$

The crystals were nucleated at a high supersaturation ($\Delta\mu/kT \approx 0.052$), and after nucleation the crystals were allowed to grow for some days at very low supersaturation ($\Delta\mu/kT < 0.002$). Then the supersaturation was increased by a fixed rate per minute while the crystals were observed with an optical microscope.

3.2. Solution Growth. The experimental setup for solution growth is somewhat different from the vapor growth experiments. A small glass growth vessel containing the crystals is cooled in a larger vessel. This vessel is kept at constant temperature (±0.02 K) using a thermostated bath. The entire growth unit is placed on a microscope stage of a microscope equiped with a video or photo camera.[37]

Naphthalene crystals have been grown from ethanol and cyclohexane solution using the following procedure. First a saturated solution is prepared and poured out into the small crystallization vessel. An air bubble is left in the vessel to compensate for differences in volume due to thermal expansion. The glass cell is sealed off and put into the larger thermostated vessel, and the temperature is lowered until crystals nucleate. Then the temperature is increased until a single crystal is left and the equilibrium temperature is determined. Subsequently, the remaining crystal was used for the observations.

It was not possible to determine a reliable solubility enthalpy for ethanol because no reproducable solubility data could be measured. Elwenspoek et al. found the same irreproducable solubility behavior for methanol.[7] Therefore, the driving force in the solution growth experiments will be expressed as the temperature difference between the equilibium temperature and the actual growth temperature ($\Delta T = T - T_{eq}$).

3.3. Results. ***3.3.1. Vapor Growth.*** In Table 5 the results of the vapor growth experiments of naphthalene and anthracene are presented. The observed morphologies are drawn in Figure 6.

After nucleation at a supersaturation of $\Delta\mu/kT \approx 5.2\%$, the naphthalene crystals showed the {001}, {110} and {20$\bar{1}$} forms.

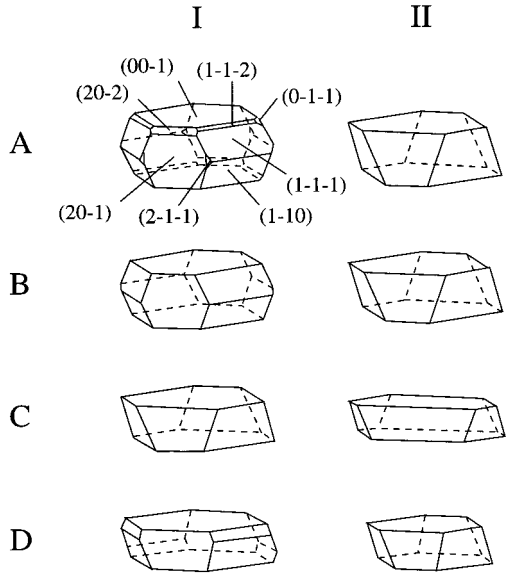

Figure 6. Experimental morphologies for naphthalene and anthracene: (I) low driving force; (II) high driving force; (A) naphthalene vapor; (B) naphthalene ethanol; (C) naphthalene cyclohexane; (D) anthracene vapor.

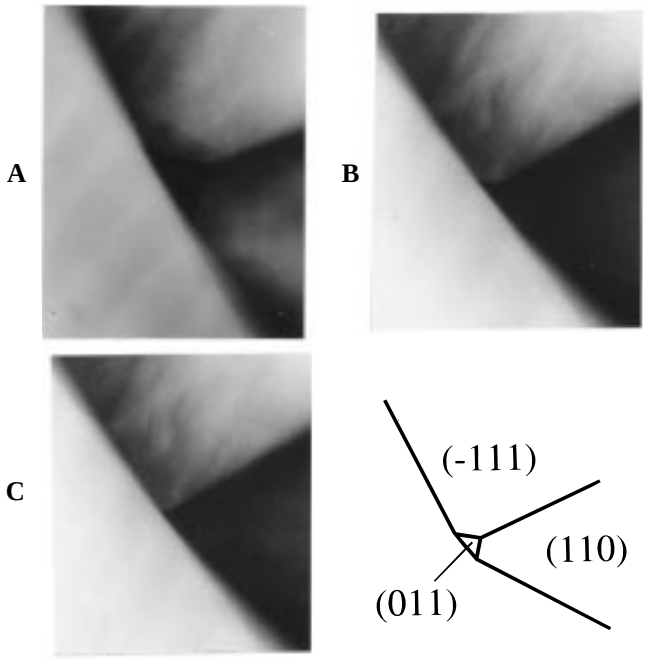

Figure 7. In situ observation of the disappearance of one of the {011} faces of a naphthalene crystal growing from the vapor at 283 K. The temperature difference ΔT at $t = 0$ was 0.4 K and was increased at 0.002 K/min. The pictures were taken at $t = 68$ (A), $t = 106$ (B), and $t = 125$ (C) min.

Most of the crystals nucleated on one of the {001} faces. The crystals were left at a very low supersaturation of approximately $\Delta\mu/kT = 0.07\%$ ($\Delta T = 0.2$ K) for several days. Then, the $\{20\bar{2}\}$, $\{1\bar{1}\bar{2}\}$, $\{2\bar{1}\bar{1}\}$, and the {011} forms developed, but these facets were not found on all crystals in the growth cell. A crystal was chosen showing {011} faces and observed by an optical microscope while the temperature of the outer wall of the growth cell was increased by 0.002 K/min. At a supersaturation of 0.2%, the (011) face disappeared rapidly from the morphology, because of a sudden increase of its relative growth rate (see Figure 7). Optically the face remained very flat during the increase in growth rate. The process was reversible. Upon decreasing the supersaturation, the (011) face reappeared on the crystal. The same phenomenon was observed for the $(11\bar{1})$ faces. These faces disappeared very quickly from the crystal morphology at a supersaturation of 3.8% and also stayed flat during the increase of the growth rate. No accurate critical supersaturations for the $\{1\bar{1}\bar{2}\}$, $\{2\bar{1}\bar{1}\}$, and $\{20\bar{2}\}$ faces have been measured. The $\{1\bar{1}\bar{2}\}$ and $\{2\bar{1}\bar{1}\}$ faces were in many cases rounded off at the edges, indicating thermal or kinetic roughening. The order of disappearance at increasing supersaturation of the above-mentioned forms is {011}, $\{2\bar{1}\bar{1}\}$,$\{1\bar{1}\bar{2}\}$, $\{20\bar{2}\}$, and $\{11\bar{1}\}$.

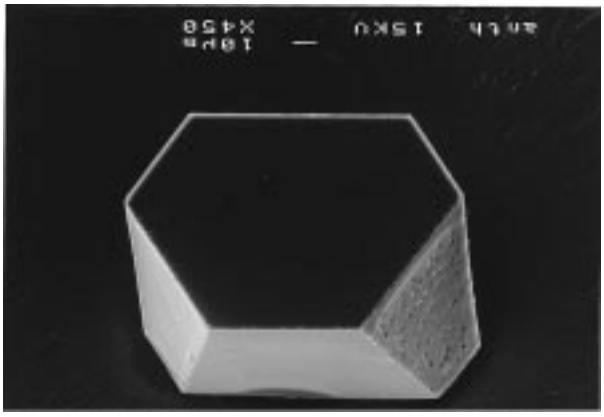

Figure 8. SEM picture of an anthracene crystal grown from the vapor at high driving force (450×, reproduced at 65% of original size).

TABLE 6: Results of the Solution Growth Experiments of Naphthalene in Ethanol and Cyclohexane. + Indicates that the Face Was Present; − Indicates That the Face Was Not Observed

	ethanol		cyclohexane	
form	low $\Delta\mu/kT$	high $\Delta\mu/kT$	low $\Delta\mu/kT$	high $\Delta\mu/kT$
$\{00\bar{1}\}$	+	+	+	+
$\{20\bar{1}\}$	+	−	+	+
$\{110\}$	+	+	+	+
$\{11\bar{1}\}$	+	−	−	−

The anthracene crystals had to be grown at a higher temperature (326.5 K) as compared to naphthalene (283.2 K), because the vapor pressure is much lower, and consequently the crystals did not grow at low temperatures. Generally, the anthracene crystals grew much slower than the naphthalene crystals. At low supersaturation, the {001}, {110}, $\{20\bar{1}\}$, and $\{11\bar{1}\}$ forms were observed, whereas at increasing supersaturation the $\{11\bar{1}\}$ faces disappeared from the morphology. The critical supersaturation at which the $\{11\bar{1}\}$ faces suddenly started to grow very rapidly is 1.8%. A SEM photo of an anthracene crystal grown from the vapor at a supersaturation higher than 1.8% is shown in Figure 8.

3.3.2. Solution Growth. The results of the solution growth experiments are summarized in Table 6. Drawings of the observed morphologies are presented in Figure 6.

At low driving forces the naphthalene crystals grown from ethanol show the {001}, $\{20\bar{1}\}$, {110}, and $\{11\bar{1}\}$ forms. At higher supersaturations ($\Delta T > 0.4$ K), the $\{11\bar{1}\}$ faces disappear, and at very high supersaturations ($\Delta T > 2.0$ K) the $\{20\bar{1}\}$ form disappears. The undercoolings at which the $\{11\bar{1}\}$ disappeared from the morphology are listed in Table 7. For the $\{20\bar{1}\}$ form no quantitative measurements were done, because the results could not be reproduced. The morphological importance of the $\{20\bar{1}\}$ faces appeared to depend on the driving force at which crystals were nucleated. When the crystals were nucleated at high driving forces ($\Delta T > 10$ K), the $\{20\bar{1}\}$ was hardly

TABLE 7: Critical Undercooling for the {11$\bar{1}$} Faces of Naphthalene Grown from Ethanol

T_{eq} (K)	ΔT (K)
291.3	0.4
289.4	1.0
284.2	2.0

observed, whereas at lower driving forces ($\Delta T = 0.2-2$ K) the {20$\bar{1}$} became more important. This may be attributed to dislocation formation at high driving forces.

When naphthalene crystals were grown from cyclohexane solution, only the {001}, {110}, and {20$\bar{1}$} faces were observed. At low driving force ($\Delta T = 0.05-0.1$ K, $T_{eq} = 290$ K) the crystals had a hexagon-like shape. At higher supersaturations ($\Delta T = 0.6$ K, $T_{eq} = 290$ K), the {20$\bar{1}$} became very important and the crystals became needle shaped. The same morphology has been reported for naphthalene crystals grown from *n*-hexane solution.[7]

4. Discussion

The theoretical morphologies based on the attachment energies (eq 3) of naphthalene and anthracene are in good agreement with the experimentally observed crystal habits. The predicted faces based on attachment energies are for both naphthalene and anthracene {001}, {20$\bar{1}$}, {110}, {11$\bar{1}$}, and {011}. All these faces have been observed on naphthalene crystals grown from the vapor at low supersaturation and, except for {011}, also on anthracene crystals.

The {020} faces have neither for naphthalene nor for anthracene been observed. This is in agreement with the theory, because these faces have a roughening temperature of 207 and 202 K for naphthalene and anthracene, respectively, which is lower than the temperature at which the crystals were grown (283 and 326 K, respectively).

Another form that occurred neither on naphthalene nor on anthracene crystals was {200}. The attachment energy of this form is very close to the threshold value for appearance in the Wulff plot, and the Ising temperature is higher than the actual growth temperature. Therefore it is expected that this form may be observed on crystals at equilibrium conditions. For naphthalene the {200} form was also not found by Pavlovska and Nenow.[4] Robinson and Scott reported the {200} form for anthracene crystals grown from the vapor.[5]

For the naphthalene crystals grown from the vapor, the {1$\bar{1}\bar{2}$} form has been found on some crystals at very low supersaturations and equilibrium conditions. According to the connected net analysis, this form is not an F-form, because no connected net (1$\bar{1}\bar{2}$) has been found. However, addition of a very weak bond u ($M_1[000]-M_1[111]$, $E^{bb} = 0.142$ kcal/mol $\approx 0.25\ kT$) to the crystal graph will make the {1$\bar{1}\bar{2}$} form an F-form. The single connected net thus found consists of the very strong q bond and the added weak bond u. The 2-D Ising temperature of the {1$\bar{1}\bar{2}$} connected nets is 379 K. The attachment energy for the {1$\bar{1}\bar{2}$} faces is -27.4 kcal/mol. With this attachment energy the form is not present on the theoretical growth form. This example clearly demonstrates that it is very important to include even weak bonds in the crystal graph in order to find all possible F-faces having a roughening temperature larger than the actual growth temperature. In general, crystal faces containing a connected net consisting of a very strong DC $[uvw]_1$ and a very weak intersecting nonparallel DC $[uvw]_2$ still have a rather high 2-D Ising transition temperature as long as the anisotropy is not too large.[3,38] These types of face may occur on crystals at equilibrium conditions as flat faces.

The most striking result of this work is the observation and growth behavior of the {011} faces on naphthalene crystals. To our knowledge these faces have only been observed by Pavlovska and Nenow for naphthalene crystals grown from the vapor at room temperature and left under equilibrium conditions for one month.[4] In section 2.3 it has been shown that, because of the presence of two symmetry-related connected nets corresponding to slightly different surfaces, the {011} faces have a very low effective step free energy according to eq 1. Consequently, the faces will have a low roughening temperature and a high growth rate due to a low 2-D nucleation barrier. The fact that the growth rate of the {011} faces drastically increased beyond a threshold supersaturation of 0.2% can be explained by this low nucleation barrier. The growth behavior of crystal faces containing multiple connected nets as compared to faces with a single connected net is the subject of a forthcoming paper.[3] When the {011} faces started to grow, no indication of a roughening effect was observed. The crystal face grew very fast as a flat face and disappeared from the morphology because of the high growth rate compared to the adjacent faces. It can be concluded that the {011} faces have a roughening temperature larger than the growth temperature of 283.2 K. At higher growth temperatures ($T > 285$ K) the {011} form has not been observed probably because this temperature is higher than the actual roughening temperature for the {011} form or due to a very small barrier for kinetic roughening.

In the case of anthracene the {011} form is not found, probably because the crystals are grown at higher temperatures due to the larger lattice energy. Therefore, the step free energy (γ) will be relatively low, resulting in a high growth rate at very low supersaturation. Alternatively, the face could already be rough at the actual experimental growth temperature. This form was also not observed by Robinson et al. on anthracene crystals grown from the vapor.[5] They observed the {001}, {20$\bar{1}$}, {110}, {11$\bar{1}$}, {011}, {20$\bar{2}$}, {11$\bar{2}$}, and {200} forms, which are all valid F-forms (see Table 4).

The {2$\bar{1}\bar{1}$} faces have the same topology as the {011} faces and also contain two symmetry-related connected nets. They have been observed as very tiny rounded-off faces on some naphthalene crystals and never on anthracene crystals. This is in agreement with the very low step free energy giving rise to a very low roughening temperature and a high growth rate. For both the {011} and {2$\bar{1}\bar{1}$} forms, the calculated 2-D Ising transition temperature is not a good estimate for the actual roughening temperature of the crystal face, because of the presence of multiple connected nets.

The {11$\bar{1}$} form contains a single connected net. However, at higher driving forces the face disappears from the morphology due to an increased growth rate. This behavior has been found for naphthalene crystals grown from the vapor and from ethanol and for anthracene crystals grown from the vapor. It is not possible to explain these observations from the connected net structure. Comparison of the {110} and {11$\bar{1}$} connected nets shows that these orientations have the same type of connected net and almost the same attachment energy and Ising transition temperature (see Tables 3 and 4). It is expected that these faces have similar growth behavior at moderate supersaturations. It has been shown that very high supersaturations tend to produce more extreme crystal habits.[18] It is expected that the faces having the lowest attachment energy and the largest d_{hkl} will become dominant. For {11$\bar{1}$} and {110}, $d_{11\bar{1}} > d_{110}$ and $E^{att}_{11\bar{1}} > E^{att}_{110}$. The {11$\bar{1}$} form will become less important at higher supersaturations, which is confirmed by the experimental

results. However, we are not able to explain the large increase in growth rate for the $\{11\bar{1}\}$ faces as compared to the $\{110\}$ faces at such a low driving force completely.

Note that looking at the order of disappearance of the crystal faces at increasing supersaturation the faces containing multiple connected nets disappeared from the morphology at the lowest driving forces.

Comparing the observed morphologies of naphthalene grown from solution or from vapor, it can be concluded that in solution fewer faces occur. This can be attributed to a lowering of the effective bond energies. The bond energies used in this paper to calculate the 2-D Ising transition temperatures T^{C}_{hkl} are bond energies Φ_i calculated in the bulk structure. Addition of all these bonds yields the sublimation enthalpy:

$$\sum_i \Phi_i = \Delta H_{\mathrm{subl}} \tag{5}$$

The bond energies for a crystal grown from solution are

$$\sum_i \Phi_i = \Delta H_{\mathrm{diss}} \tag{6}$$

The 2-D Ising transition temperatures in solution can be roughly estimated by[14]

$$T^{\mathrm{C}}_{\mathrm{solution}} = \frac{\Delta H_{\mathrm{diss}}}{\Delta H_{\mathrm{subl}}} T^{\mathrm{C}}_{\mathrm{calc}} \tag{7}$$

In general, dissolution enthalpies are lower than the sublimation enthalpies. This implies that the Ising transition temperatures will be lower in solution. A lowering of the transition temperature also implies that the step free energy will be lower, resulting in a low barrier for kinetic roughening. Consequently, fewer faces will occur on crystals grown from solution as compared to crystals grown from the vapor. Using the dissolution enthaply of naphthalene in *n*-hexane $\Delta H^{n-\mathrm{hex}}_{\mathrm{diss}} = 7.9$ kcal/mol[7] and the sublimation enthalpy of naphthalene $\Delta H_{\mathrm{subl}} = 17.4$ kcal/mol, the roughening temperatures in Table 3 have to be multiplied by a factor 0.45 according to eq 7. The corrected 2-D Ising transition temperatures of the faces in Table 3 are $\{001\}$ ($T^{\mathrm{C}}_{n-\mathrm{hex}} = 831$ K), $\{110\}$ ($T^{\mathrm{C}}_{n-\mathrm{hex}} = 434$ K), $\{20\bar{1}\}$ ($T^{\mathrm{C}}_{n-\mathrm{hex}} = 386$ K), $\{11\bar{1}\}$ ($T^{\mathrm{C}}_{n-\mathrm{hex}} = 405$ K), $\{011\}$ ($T^{\mathrm{C}}_{n-\mathrm{hex}} = 266$ K), $\{200\}$ ($T^{\mathrm{C}}_{n-\mathrm{hex}} = 224$ K), $\{20\bar{2}\}$ ($T^{\mathrm{C}}_{n-\mathrm{hex}} = 190$ K), $\{2\bar{1}\bar{1}\}$ ($T^{\mathrm{C}}_{n-\mathrm{hex}} = 167$ K), and $\{020\}$ ($T^{\mathrm{C}}_{n-\mathrm{hex}} = 93$ K). The Ising temperatures of the last five faces are lower than the actual experimental growth temperature. Therefore these facets are not expected to occur on the morphology of naphthalene crystals grown from *n*-hexane solution. This theoretical result is confirmed by Elwenspoek et al.[7] The result of *n*-hexane may be comparable to our results for cyclohexane. The experimental results for cyclohexane show that none of the above-mentioned faces having a very low Ising temperature occur on the morphology. Anomalies can be expected in the case where solvent has a special interaction with a specific crystal face (*hkl*), as then eq 7 does not hold.[7,39]

5. Conclusions

In this paper we have shown that the morphology of naphthalene and anthracene crystals depends strongly on the applied driving force, temperature, and mother phase. The connected net analysis combined with Ising transition temperature and attachment energy calculations predicts the most important faces observed on experimentally grown crystals. However, the attachment energy prediction of the growth morphology does not take the influence of a mother phase, driving force, and symmetry-related pairs of connected nets into account. For specific orientations having multiple connected nets the attachment energy is not a good parameter for the relative growth rate.

We have found experimental evidence that the $\{011\}$ and $\{2\bar{1}\bar{1}\}$ faces have a very low step free energy, which is attributed to a pair of connected nets giving rise to a zero step energy (symmetry roughening) in the broken bond approximation. However, because of the different molecular structure at the interfaces corresponding to the two connected nets, the step free energy will be larger than zero, but very low. Experimentally the $\{011\}$ faces have been observed on naphthalene crystals at very low supersaturation and disappear from the morphology rapidly beyond a threshold supersaturation due to an increase in relative growth rate. This is attributed to the presence of a symmetry-related pair of connected nets causing a low 2-D nucleation barrier. In our opinion this example demonstrates the importance of determining all connected nets of a crystal structure in order to understand the growth behavior. Moreover, it has been shown that the standard attachment energy method to determine the morphological importance of a crystal face (*hkl*) fails for faces containing a pair of connected nets giving rise to a very low step free energy in spite of a low attachment energy.

The connected net structure of the $\{11\bar{1}\}$ faces is almost equal to that of the $\{110\}$ faces. Nevertheless, the $\{11\bar{1}\}$ faces show an increased growth rate as compared to the $\{110\}$ faces at higher supersaturations. This cannot be explained by the connected net analysis. However, this is another example that the attachment energy description of relative growth rates of crystal faces does not hold in general.

Observation of the $\{1\bar{1}\bar{2}\}$ faces demonstrates that it is important to include even very weak bonds in the connected net analysis in order to determine all faces with a roughening temperature above the actual growth temperature.

Finally, the morphologies of naphthalene crystals grown from solution exhibit fewer faces as compared to vapor-grown crystals. This can be attributed to a lowering of the effective bond energies at the crystal-mother phase interface, resulting in a lower roughening temperature and thus a higher growth rate.

Acknowledgment. R.F.P.G. would like to acknowledge the financial support of the Dutch Organisation of Technical Sciences (STW).

References and Notes

(1) Grimbergen, R. F. P.; Meekes, H.; Strom, C. S.; Vogels, L. J. P.; Bennema, P. *Acta Crystallogr. A*, accepted for publication.
(2) Meekes, H.; Bennema, P.; Grimbergen, R. F. P. *Acta Crystallogr. A*, accepted for publication.
(3) Grimbergen, R. F. P.; Bennema, P.; Meekes, H. To be published.
(4) Pavlovska, A.; Nenow, D. *J. Cryst. Growth* **1972**, *12*, 9−12.
(5) Robinson, P. M.; Scott, H. G. *J. Cryst. Growth* **1967**, *1*, 187−194.
(6) Jetten, L. A. M. J.; Human, H. J.; Bennema, P.; van der Eerden, J. P. *J. Cryst. Growth* **1984**, *68*, 503.
(7) Elwenspoek, M.; Bennema, P.; van der Eerden, J. P. *J. Cryst. Growth* **1987**, *83*, 297.
(8) Hartman, P.; Perdok, W. G. *Acta Crystallogr.* **1955**, *8*, 49.
(9) Hartman, P.; Perdok, W. G. *Acta Crystallogr.* **1955**, *8*, 521.
(10) Hartman, P.; Perdok, W. G. *Acta Crystallogr.* **1955**, *8*, 525.
(11) Hartman, P. In *Crystal Growth, an Introduction*; North Holland Publishing Company: Dordrecht, 1973; pp 367−402.
(12) Rijpkema, J. J. M.; Knops, H. J. F.; Bennema, P.; van der Eerden, J. P. *J. Cryst. Growth* **1982**, *61*, 295.
(13) Bennema, P.; van der Eerden, J. P. In *Morphology of Crystals*; Terra Scientific Publishing Company (TERRAPUB): Tokyo, 1987; pp 1−75.

(14) Bennema, P. In *Handbook of Crystal Growth*; Hurle, D. T. J., Ed.; Elsevier: Amsterdam, 1993; Vol. 1; Chapter 7.
(15) Friedel, G. *Leçon de Cristallographie*; Hermann: Paris, 1911.
(16) Donnay, J. D. H.; Harker, D. *Am. Mineral.* **1937**, *22*, 446.
(17) van Beijeren, H.; Nolden, I. M. In *Topics in Current Physics, Structure and Dynamics of Surfaces II*; Springer Verlag: Berlin, 1986; Vol. 43; pp 259−300.
(18) Hartman, P.; Bennema, P. *J. Cryst. Growth* **1980**, *49*, 145−156.
(19) Wulff, G. *Z. Kristallogr. Miner.* **1901**, *34*, 449.
(20) Grimbergen, R. F. P.; Meekes, H.; Boerrigter, S. X. M. C-program FACELIFT for PBC analysis, Dept. of Solid State Chemistry, University of Nijmegen, 1997.
(21) Strom, C. S. *Z. Kristallogr.* **1980**, *153*, 99.
(22) Strom, C. S. *Z. Kristallogr.* **1981**, *154*, 31.
(23) Strom, C. S. *Z. Kristallogr.* **1985**, *172*, 11.
(24) Guest, M. F.; Kendrick, J.; van Lenthe, J. H.; van Schoeffel, K.; Sherwood, P. *GAMESS-UK Users Guide and Reference Manual*; Computing for Science (CFS) Ltd.: Daresbury Laboratory, 1994.
(25) Schaftenaar, G. *QCPE Bull.* **1992**, *12*, 3.
(26) Besler, B. H.; Merz, K. M.; Kollman, P. A. *J. Comput. Chem.* **1990**, *11*, 431−439.
(27) Cerius^2 software version 3.0; Biosym/Molecular Simulations Inc.: San Diego, CA, 1997.
(28) Hoeks, B. C-program TCRITIC, program for calculating roughening temperatures, Dept. of Solid State Chemistry, University of Nijmegen, 1993.
(29) Brock, C. P.; Dunitz, J. D. *Acta Crystallogr. B* **1982**, *38*, 2218.
(30) Brock, C. P.; Dunitz, J. D. *Acta Crystallogr. B* **1990**, *46*, 795.
(31) *International Tables for X-Ray Crystallography*; The Kynoch Press: Birmingham, England, 1969; Vol. 1.
(32) Hartman, P. *J. Cryst. Growth* **1991**, *110*, 559.
(33) Docherty, R.; Clydesdale, G.; Roberts, K. J.; Bennema, P. *J. of Phys. D: Appl. Phys.* **1991**, *24*, 89.
(34) Berkovitch-Yellin, Z. J. *J. Am. Chem. Soc.* **1985**, *107*, 8239.
(35) Hartman, P.; Heijnen, W. M. M. *J. Cryst. Growth* **1983**, *63*, 261−264.
(36) van Leeuwen, C. *J. Cryst. Growth* **1979**, *46*, 91.
(37) Vogels, L. J. P.; Marsman, H. A. M.; Verheijen, M. A. *J. Cryst. Growth* **1990**, *100*, 439.
(38) Burton, W. K.; Cabrera, N.; Frank, C. F. *Trans. R. Soc. A* **1951**, *243*, 299.
(39) Shekunov, B. Y.; Latham, R. J. *J. Phys. Chem.* **1996**, *100*, 5464.